Type Ia Supernova nucleosynthesis

10th Russbach School on Nuclear Astrophysics

Russbach, March 12, 2013

Ivo Rolf Seitenzahl

Institut für Theoretische Physik und Astrophysik

Julius-Maximilians-Universität Würzburg

Main collaborators for this work: F. Ciaraldi-Schoolmann, M. Fink, W. Hillebrandt, M. Kromer, R. Pakmor, F. Röpke, A. Ruiter, S. Sim, S.Taubenberger, C. Travaglio

Emmy Noether Research Group

SN Ia

Explosive nucleosynthesis

- Thermonuclear fusion in supernovae does not proceed under hydrostatic conditions, rather in a rapidly expanding medium.
- Often temperatures reached are high enough that reaction rates are so fast that nuclear statistical equilibrium (NSE) is reached. Y_e~0.5

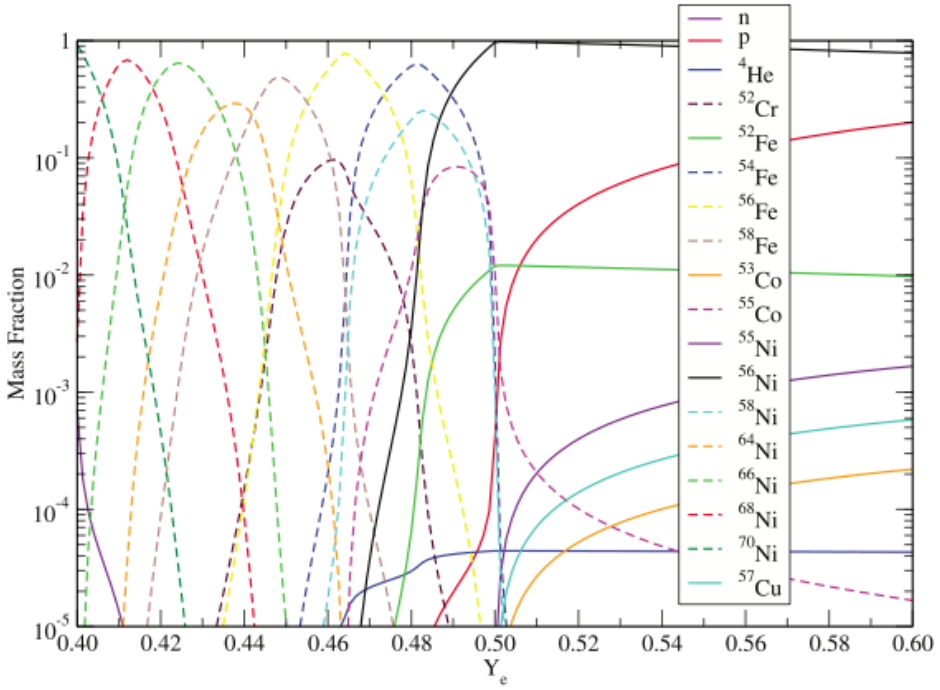

- In NSE, all nuclear reactions are in detailed balance, and the equilibrium mass fractions are determined by minimizing the Helmholtz free energy F=(U-Q)-TS.

→ High entropy environments are dominated by light particles (such as p,n,^{4}He).

- → Low entropy environments are dominated by nuclei with the highest binding energy for the given neutron excess (here: Fe-group).

Seitenzahl et al. (2008) ApJ 685, L129

Example: nucleosynthesis conditions in SNe Ia

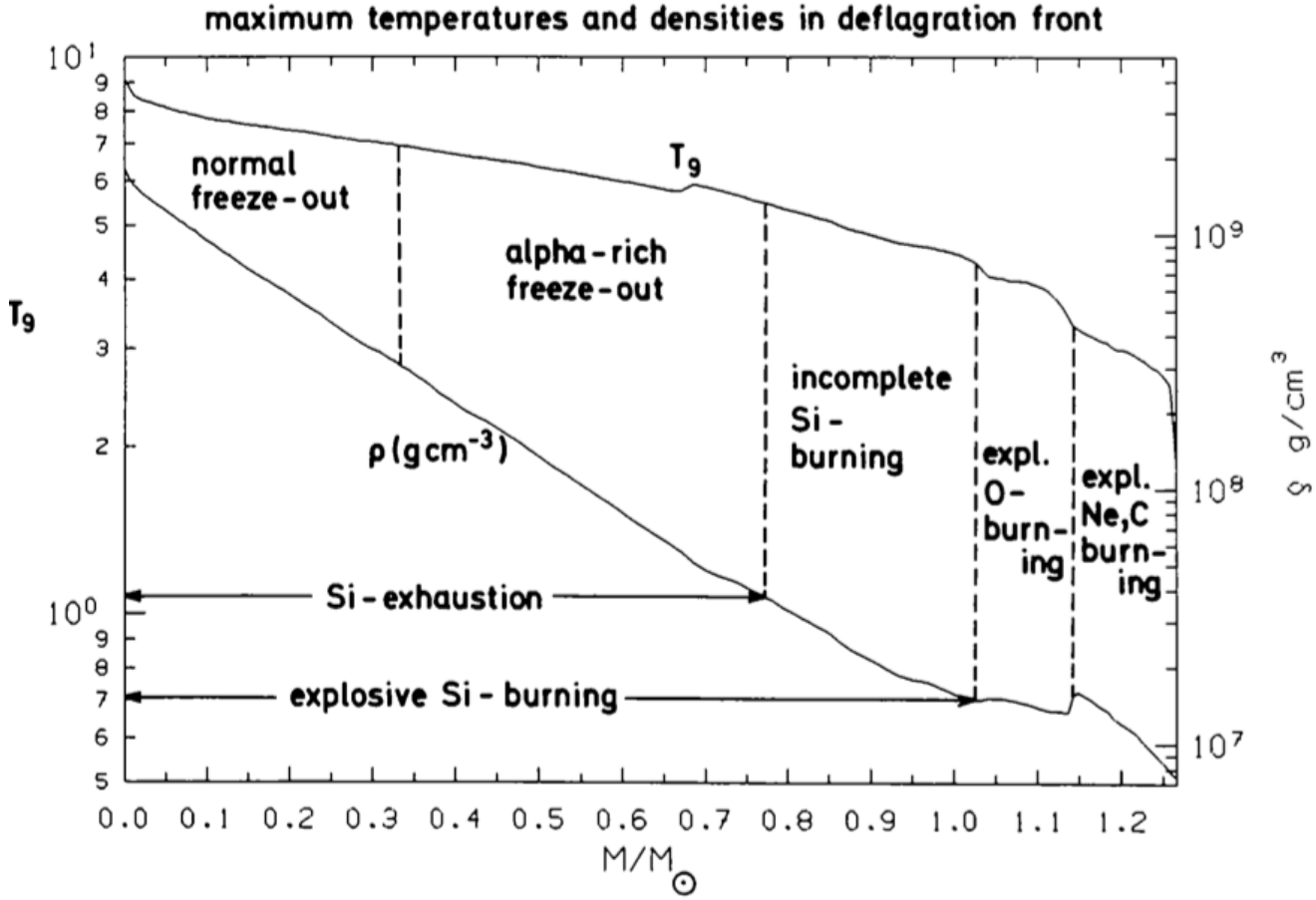

Thielemann et al. 1986

Normal freeze-out from NSE:

- Lower entropy, higher densities > 3e8 g cm^{-3}
- Low light particle fraction during freeze-out
- ^{55}Co survives

Alpha-rich freeze-out from NSE

- Higher entropy, lower densities < 3e8 g cm^{-3}
- High light particle fraction during freeze-out
- ^{55}Co destroyed by ^{55}Co(p,γ)^{56}Ni

Example: nucleosynthesis conditions in SNe Ia

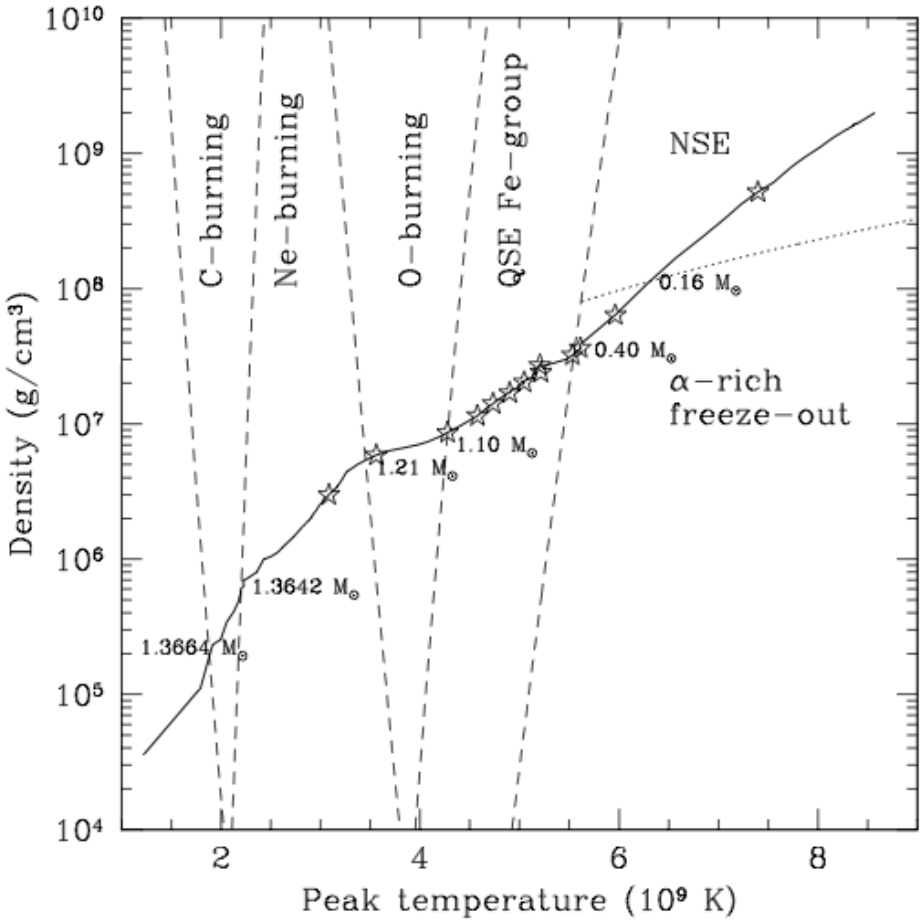

Bravo, Martinez-Pinedo 2012

Normal freeze-out from NSE:

- Lower entropy, higher densities > 3e8 g cm^{-3}
- Low light particle fraction during freeze-out
- ^{55}Co survives

Alpha-rich freeze-out from NSE

- Higher entropy, lower densities < 3e8 g cm^{-3}
- High light particle fraction during freeze-out
- ^{55}Co destroyed by ^{55}Co(p,γ)^{56}Ni

Nucleosynthesis with tracer particles

Treatment of nucleosynthesis

- approximate description of burning in hydro simulations to capture energetics since full network coupled to hydro still computationally not feasible in 3D
- large number of mass-less tracer particles (typically 1 million for 3D simulations) distributed in the initial model
- each particle generally represents a mass m_i
- particles get advected by the flow and record as a function of time the local thermodynamic conditions
- yields are obtained by post-processing these trajectories by a large nuclear reaction network, including weak interactions (electron captures, beta decays)

(MPA results are based on Thielemann's nuclear network code, Basel reaction rate library)

Tracer particle distributions

- Tracer particle positions 100s after the explosion colored by Ni56 mass fraction
- Spherical cloud of tracers was cut in half (bottom) and then rotated 90 degrees (right) to allow view deep into the core

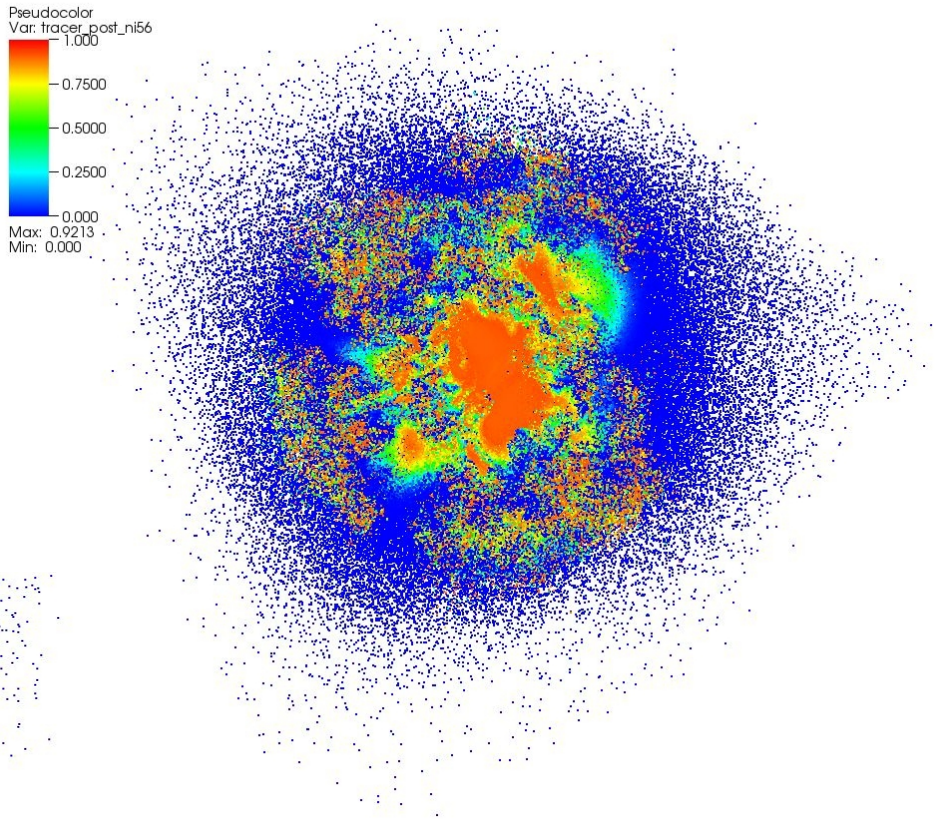

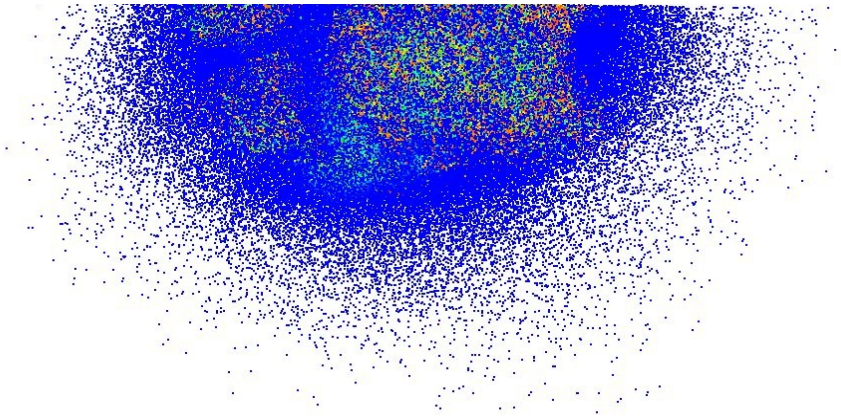

Abundance evolution along tracer trajectory

- Contrary to nuclear fusion in the Sun, the burning is not hydrostatic, but rather "explosive" → temperature rises due to nuclear burn, but then decreases exponentially due to subsequent expansion
- Important to follow isotopic evolution throughout freeze-out phase, when reaction rates become too slow to keep abundances in equilibrium corresponding to thermodynamic state

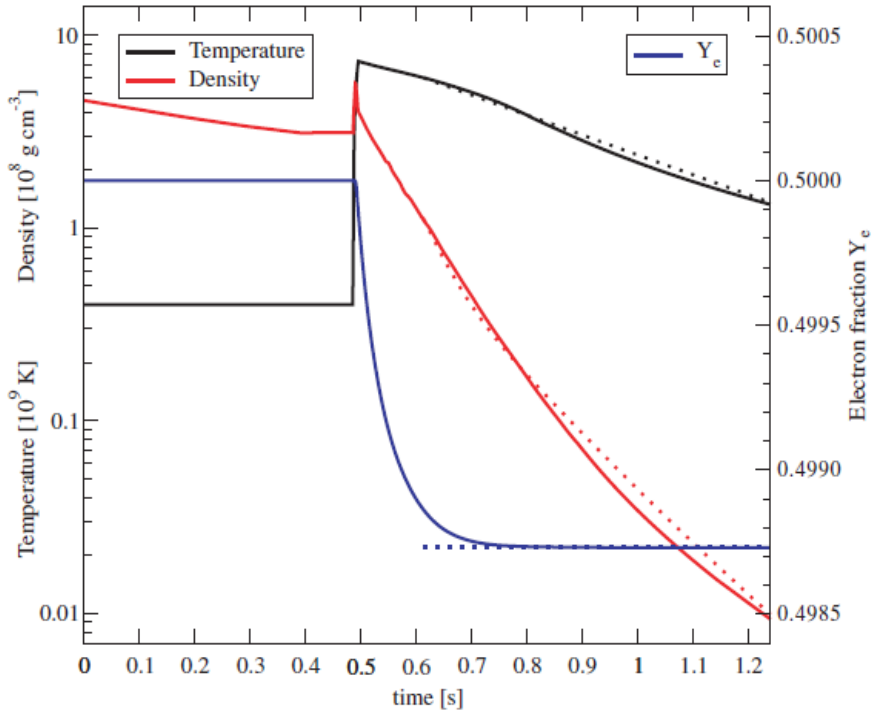

Meakin, Seitenzahl et al. (2011) ApJ 693, 1188

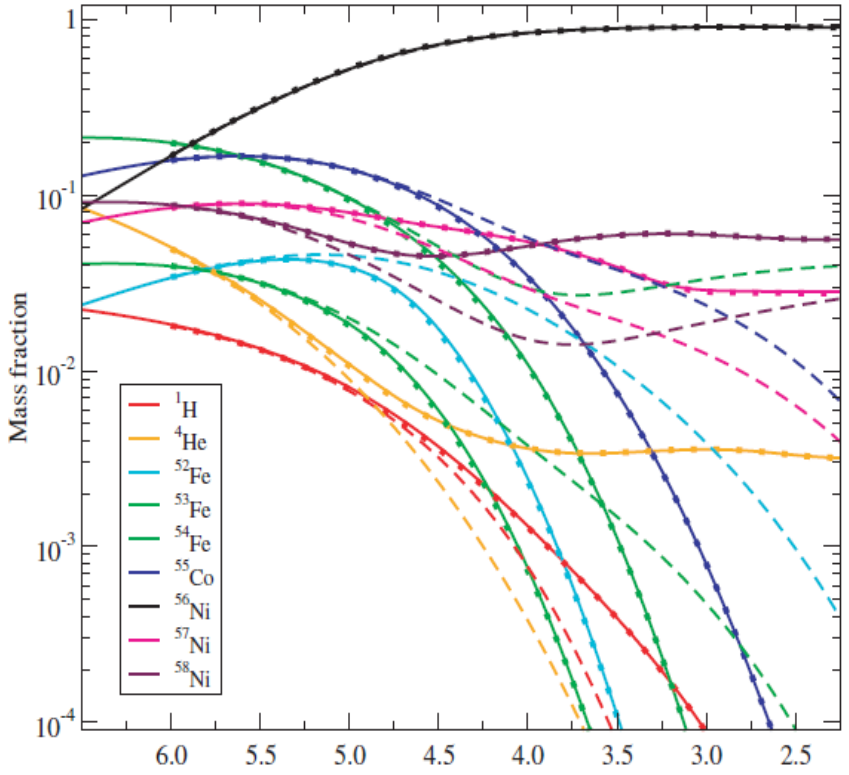

Abundance evolution along tracer trajectory movie

New 3D delayed detonation SNe Ia yield tables

Table 2. Asymptotic nucleosynthetic yields (in solar masses) of stable nuclides.

	N1	N3	N5	N10	N20	N40	N100H	N100	N100L	N150	N200	N300C	N1600	N1600C	N100_Z0.5	N100_Z0.1	N100_Z0.01
^{12}C	2.61E-03	9.90E-03	9.05E-03	4.43E-03	9.20E-03	3.90E-03	3.87E-03	3.04E-03	3.85E-03	1.72E-02	1.21E-02	8.86E-03	1.06E-02	1.68E-02	3.10e-03	3.15e-03	3.16e-03
^{13}C	1.84E-08	6.15E-08	5.05E-08	2.57E-08	4.52E-08	2.18E-08	2.28E-08	1.74E-08	2.17E-08	1.00E-07	6.57E-08	4.95E-08	5.57E-08	8.44E-08	8.47e-09	1.91e-09	2.72e-10
^{14}N	2.92E-06	9.93E-06	8.46E-06	3.85E-06	8.34E-06	4.30E-06	4.25E-06	3.21E-06	3.98E-06	1.84E-05	1.33E-05	9.16E-06	1.04E-05	1.88E-05	1.80e-06	4.71e-07	7.22e-08
^{15}N	3.36E-09	1.22E-08	1.03E-08	4.47E-09	1.03E-08	5.16E-09	5.24E-09	3.67E-09	4.66E-09	2.29E-08	1.71E-08	1.14E-08	1.29E-08	2.41E-08	2.07e-09	2.98e-09	8.73e-08
^{16}O	2.63E-02	4.74E-02	5.63E-02	5.16E-02	9.04E-02	9.89E-02	7.30E-02	1.01E-01	1.24E-01	1.24E-01	1.96E-01	1.21E-01	1.91E-01	2.72E-01	9.87e-02	9.64e-02	9.47e-02
^{17}O	3.96E-07	1.37E-06	1.16E-06	5.34E-07	1.12E-06	5.54E-07	5.61E-07	4.13E-07	5.14E-07	2.48E-06	1.74E-06	1.22E-06	1.36E-06	2.42E-06	2.84e-07	9.32e-08	5.43e-09
^{18}O	3.32E-09	1.33E-08	1.11E-08	4.54E-09	1.12E-08	5.29E-09	5.59E-09	3.53E-09	4.61E-09	2.52E-08	1.98E-08	1.25E-08	1.44E-08	2.73E-08	2.23e-09	1.21e-09	9.93e-10
^{19}F	3.73E-11	1.35E-10	1.17E-10	5.05E-11	1.22E-10	6.22E-11	6.32E-11	4.39E-11	5.68E-11	2.64E-10	2.13E-10	1.36E-10	1.58E-10	2.97E-10	2.20e-11	1.48e-1	4.79e-11
^{20}Ne	1.47E-03	3.37E-03	3.75E-03	2.40E-03	5.41E-03	4.15E-03	3.66E-03	3.53E-03	4.33E-03	8.72E-03	1.15E-02	6.76E-03	9.40E-03	1.73E-02	3.60e-03	3.69e-0	3.74e-03
^{21}Ne	3.08E-07	9.79E-07	8.81E-07	4.16E-07	9.63E-07	5.43E-07	5.20E-07	4.11E-07	5.17E-07	1.98E-06	1.68E-06	1.08E-06	1.29E-06	2.39E-06	1.97e-07	4.47e-08	6.93e-09
^{22}Ne	6.40E-05	3.26E-04	2.87E-04	1.31E-04	2.58E-04	5.77E-05	7.62E-05	4.07E-05	5.51E-05	4.83E-04	2.34E-04	2.11E-04	2.32E-04	2.97E-04	1.65e-05	2.30e-06	1.71e-07
^{23}Na	2.20E-05	6.41E-05	6.09E-05	3.22E-05	7.30E-05	4.66E-05	4.25E-05	3.74E-05	4.68E-05	1.38E-04	1.38E-04	8.53E-05	1.09E-04	2.03E-04	2.63e-05	1.96e-05	1.72e-05
^{24}Mg	3.93E-03	7.13E-03	8.53E-03	7.77E-03	1.46E-02	1.54E-02	1.15E-02	1.52E-02	1.83E-02	1.93E-02	3.32E-02	1.97E-02	3.08E-02	4.61E-02	2.02e-02	2.69e-02	2.90e-02
^{25}Mg	3.35E-05	9.26E-05	8.92E-05	5.07E-05	1.11E-04	7.70E-05	6.86E-05	6.49E-05	8.02E-05	2.02E-04	2.14E-04	1.33E-04	1.75E-04	3.12E-04	3.09e-05	1.06e-05	8.99e-07
^{26}Mg	5.15E-05	1.36E-04	1.34E-04	7.55E-05	1.71E-04	1.17E-04	1.04E-04	9.66E-05	1.19E-04	3.07E-04	3.27E-04	2.01E-04	2.62E-04	4.82E-04	4.44e-05	7.36e-06	1.04e-06
^{27}Al	1.98E-04	3.95E-04	4.56E-04	3.71E-04	7.32E-04	7.05E-04	5.47E-04	6.74E-04	8.32E-04	1.04E-03	1.[illegible]E-03	7.68E-04	1.48E-03	2.37E-03	5.88e-04	2.68e-04	8.71e-05
^{28}Si	6.32E-02	8.99E-02	1.19E-01	1.38E-01	1.98E-01	2.59E-01	2.12E-01	2.84E-01	3.55E-01	2.71E-01	2.[illegible]E-01	3.19E-01	3.61E-01	3.44E-01	2.90e-01	2.94e-01	2.89e-01
^{29}Si	2.69E-04	4.64E-04	5.68E-04	5.17E-04	9.49E-04	1.03E-03	7.73E-04	1.03E-03	1.25E-03	1.30E-[illegible]	2.[illegible]E-03	1.29E-03	1.97E-03	2.86E-03	7.28e-04	4.30e-04	1.35e-04
^{30}Si	5.96E-04	1.00E-03	1.23E-03	1.18E-03	2.12E-03	2.35E-03	1.72E-03	2.36E-03	2.86E-03	2.77E-03	4.76E-03	2.87E-03	4.53E-03	6.55E-03	1.19e-03	1.44e-04	1.84e-05
^{31}P	1.40E-04	2.28E-04	2.87E-04	2.78E-04	4.87E-04	5.60E-04	4.20E-04	5.77E-04	7.0[illegible]E-04	6.[illegible]E-04	1.08E-03	6.85E-04	1.05E-03	1.47E-03	3.58e-04	1.05e-04	3.54e-05
^{32}S	2.62E-02	3.70E-02	4.79E-02	5.74E-02	7.74E-02	1.01E-01	8.55E-02	1.11E-[illegible]	1.38E-01	1.07E-01	1.10E-01	1.27E-01	1.22E-01	1.03E-01	1.12e-01	1.12e-01	1.15e-01
^{33}S	7.51E-05	1.06E-04	1.42E-04	1.53E-04	2.43E-04	3.14E-04	2.37E-04	3.39E-04	4.21E-04	3.27E-04	5.23E-04	3.65E-04	5.47E-04	6.79E-04	2.39e-04	1.04e-04	4.57e-05
^{34}S	8.26E-04	1.16E-03	1.57E-03	1.75E-03	2.84E-03	3.73E-03	2.[illegible]E-03	4.04E-03	5.02E-03	3.68E-03	6.22E-03	4.22E-03	6.56E-03	8.06E-03	1.86e-03	2.60e-04	7.14e-06
^{36}S	8.12E-08	1.35E-07	1.65E-07	1.41E-07	2.54E-07	2.[illegible]E-07	1.[illegible]E-07	2.47E-07	3.05E-07	3.59E-07	5.42E-07	3.23E-07	4.97E-07	7.68E-07	3.86e-08	1.64e-09	1.73e-11
^{35}Cl	4.29E-05	6.20E-05	8.27E-05	8.37E-05	1.35E-04	1.67E-04	1.27E-04	1.78E-04	2.27E-04	1.89E-04	2.89E-04	2.00E-04	2.98E-04	3.84E-04	9.91e-05	2.64e-05	5.65e-06
^{37}Cl	7.32E-06	9.62E-06	1.34E-05	1.53E-05	2.26E-05	3.14E-05	2.44E-05	3.51E-05	4.49E-05	3.14E-05	4.66E-05	3.63E-05	5.22E-05	5.75E-05	2.27e-05	9.14e-06	3.52e-06
^{36}Ar	4.52E-03	6.36E-03	8.03E-03	9.89E-03	1.28E-02	1.61E-02	1.43E-02	1.77E-02	2.17E-02	1.76E-02	1.50E-02	2.08E-02	1.64E-02	1.23E-02	1.85e-02	1.92e-02	2.04e-02
^{38}Ar	3.77E-04	5.15E-04	7.18E-04	8.01E-04	1.25E-03	1.72E-03	1.29E-03	1.91E-03	2.48E-03	1.69E-03	2.69E-03	1.96E-03	2.98E-03	3.42E-03	8.31e-04	1.19e-04	5.40e-06
^{40}Ar	1.68E-09	2.45E-09	1.[illegible]E-09	2.90E-09	4.79E-09	5.27E-09	3.81E-09	5.21E-09	6.60E-09	6.64E-09	1.04E-08	6.29E-09	9.87E-09	1.48E-08	4.66e-10	9.87e-12	5.11e-14
^{39}K	2.26E-05	2.98E-05	4.12E-05	4.65E-05	6.80E-05	9.52E-05	7.40E-05	1.07E-04	1.39E-04	9.53E-05	1.42E-04	1.10E-04	1.60E-04	1.75E-04	6.25e-05	1.89e-05	3.57e-06
^{41}K	1.29E-06	1.69E-06	2.30E-06	2.66E-06	3.80E-06	5.38E-06	4.22E-06	6.08E-06	7.87E-06	5.36E-06	7.81E-06	6.21E-06	8.93E-06	9.65E-06	3.85e-06	1.42e-06	4.92e-07
^{40}Ca	4.05E-03	5.74E-03	7.09E-03	8.82E-03	1.13E-02	1.35E-02	1.24E-02	1.47E-02	1.75E-02	1.50E-02	1.07E-02	1.78E-02	1.10E-02	7.50E-03	1.57e-02	1.66e-02	1.77e-02

New 3D delayed detonation SNe Ia yield tables

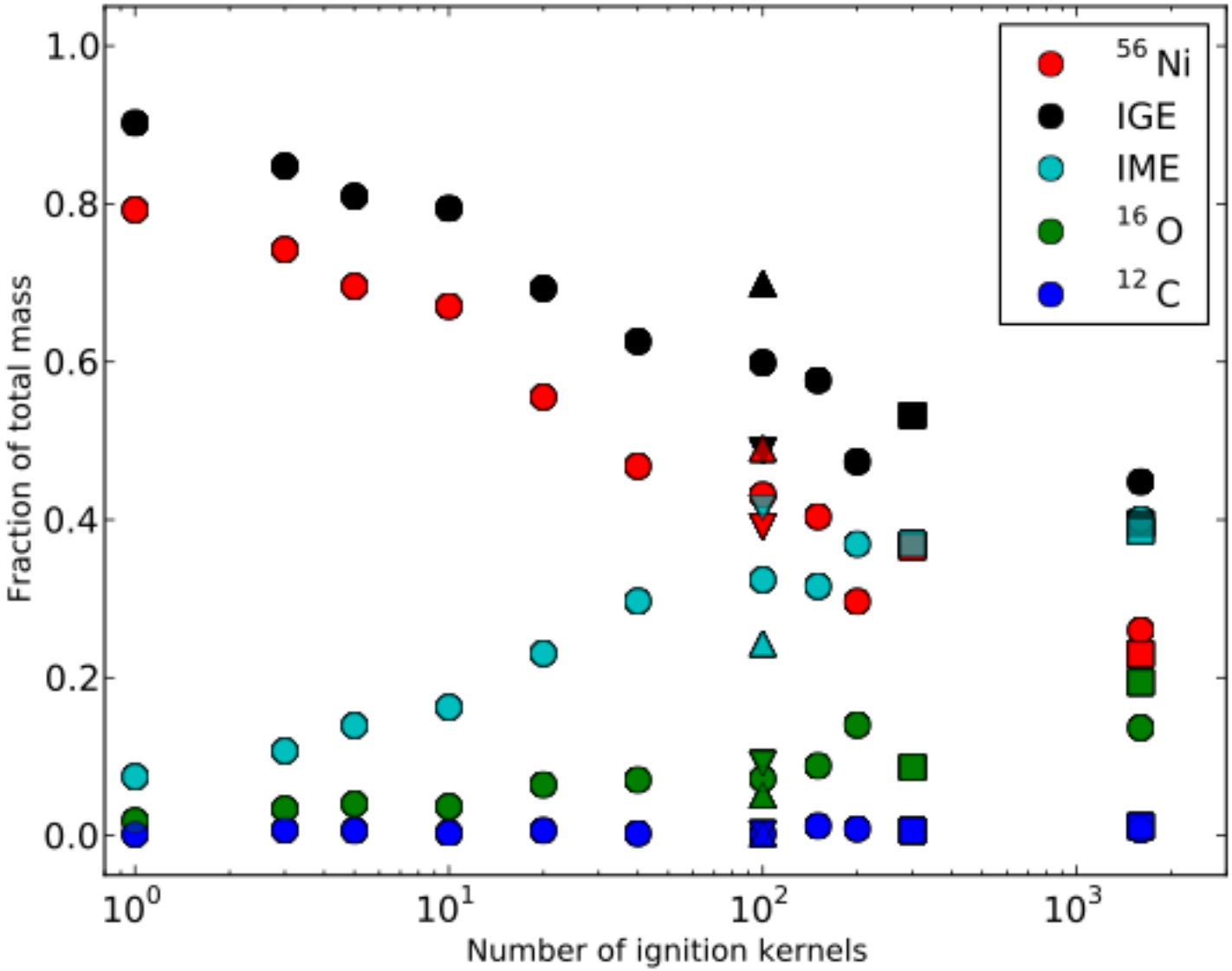

1D and 3D model yields: a qualitative comparison
W7

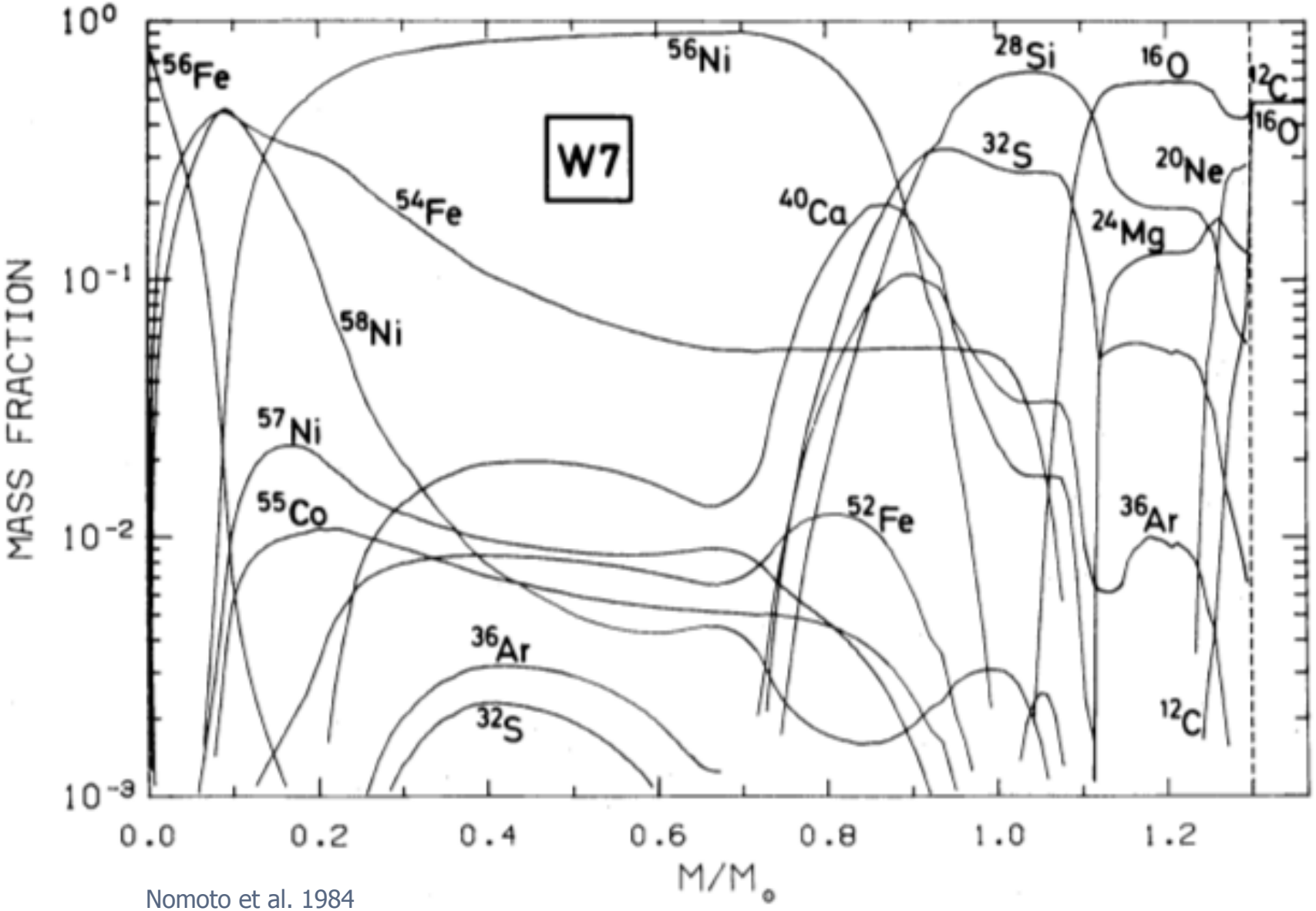

Nomoto et al. 1984

1D and 3D model yields: a qualitative comparison
N100

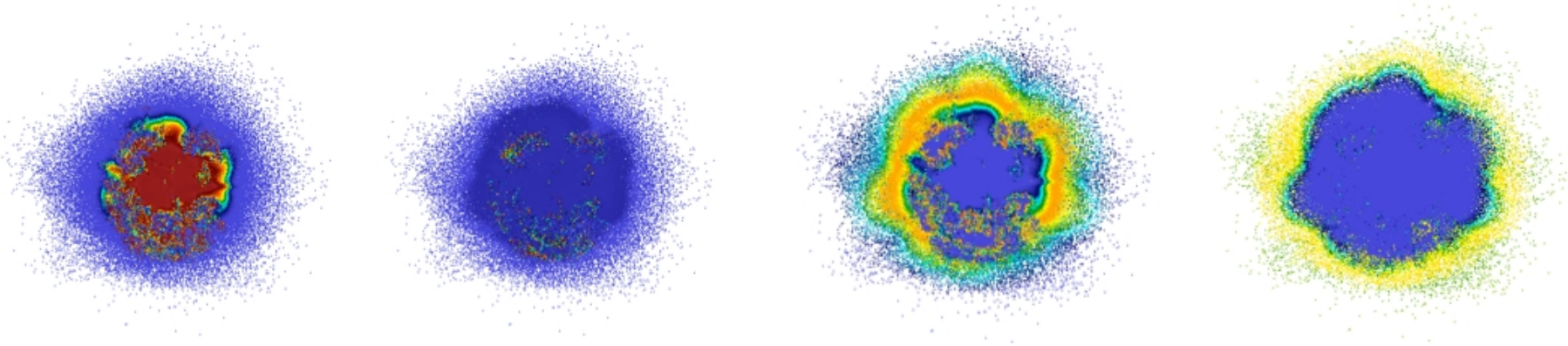

(f) N100; X(^{56}Ni) (g) X(^{54}Fe+^{56}Fe+^{58}Ni) (h) X(^{28}Si) (i) X(^{16}O)

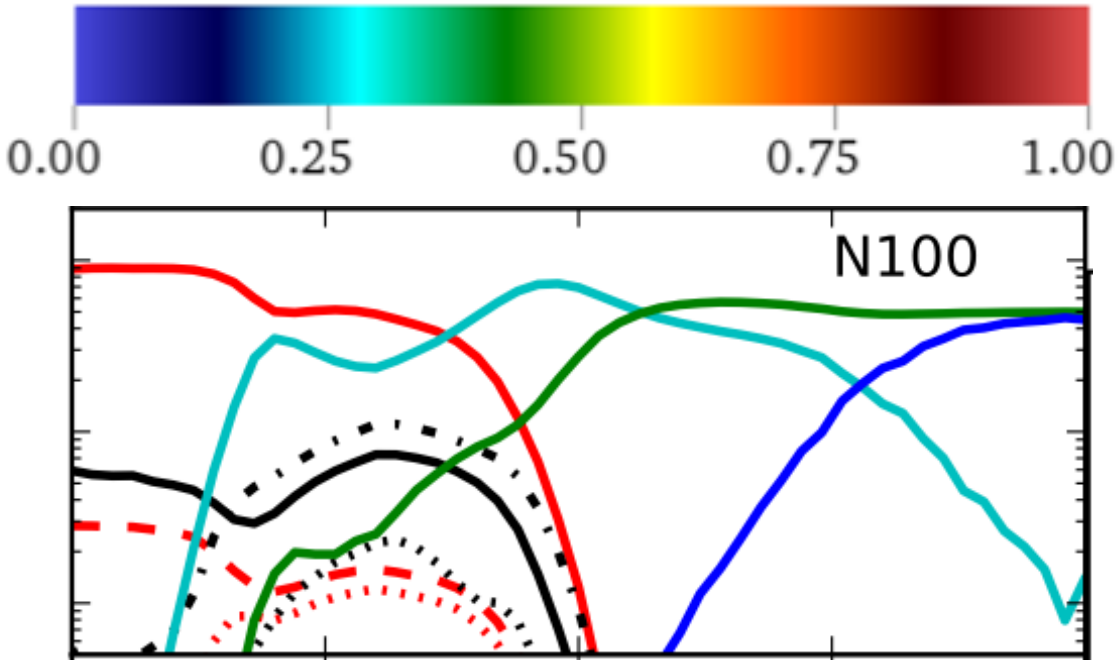

(Seitenzahl, Ciaraldi-Schoolmann, Röpke et al. 2013, MNRAS 429, 1156)

Central density dependent yields for 3D SNe Ia and overproduction of neutron rich isotopes

W7 (squares, Iwamoto 1999) with old FFN electron-capture rates, 3D delayed-detonation models N100H (high central density, upside triangles), N100 (canonical central density, circles) and N100L (low central density, downside triangles).

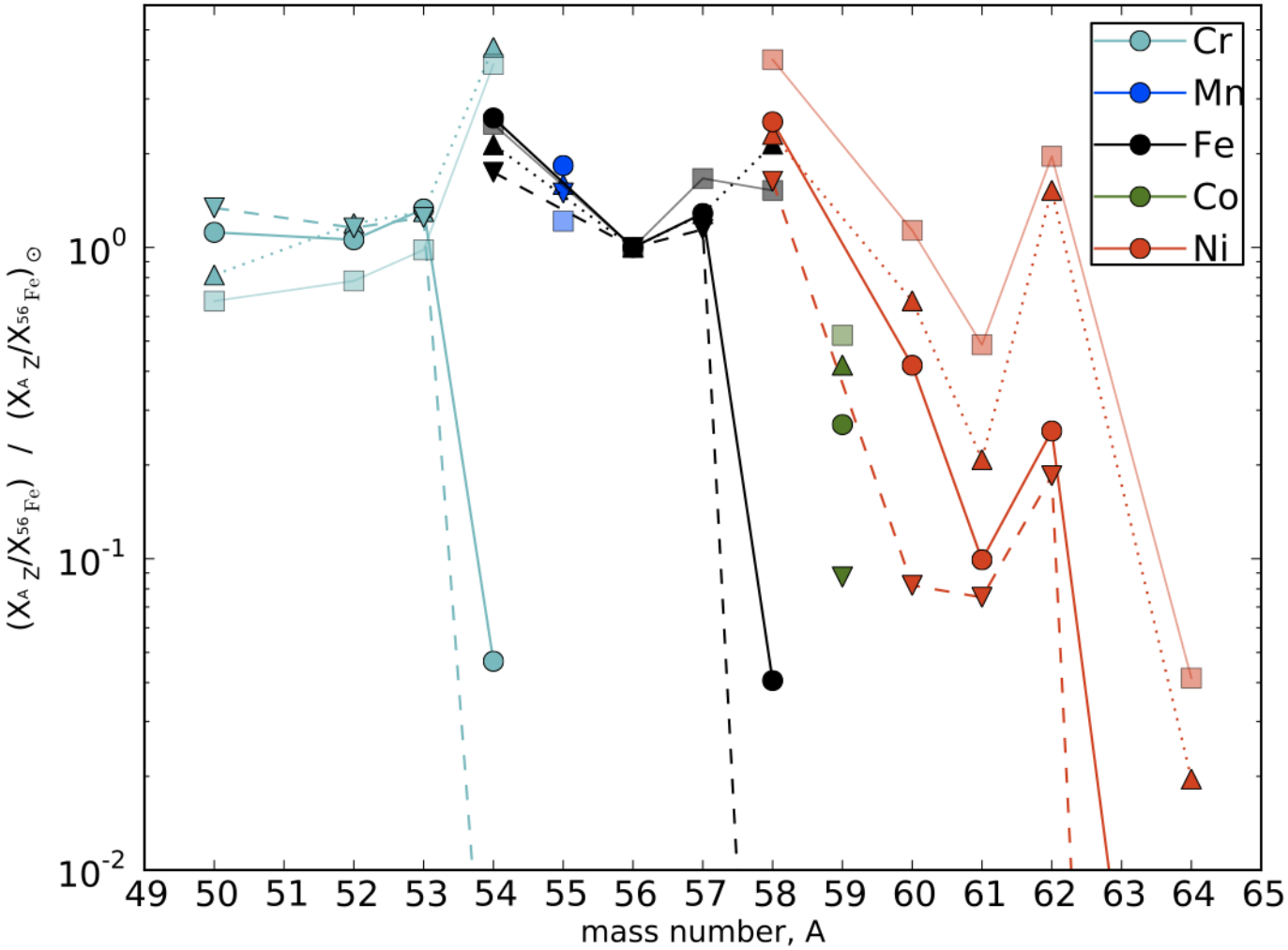

Metallicity dependent Fe-group yields for delayed-detonation 3D SNe Ia

Compared to W7 (squares, Maeda 2010), 3D delayed-detonation models produce (normalized to ^{56}Fe) different yield pattern in the Fe-peak, i.e. more Mn, less Co and Ni. Coupling different SN Ia yields to chemical evolution are one possible way to distinguish models.

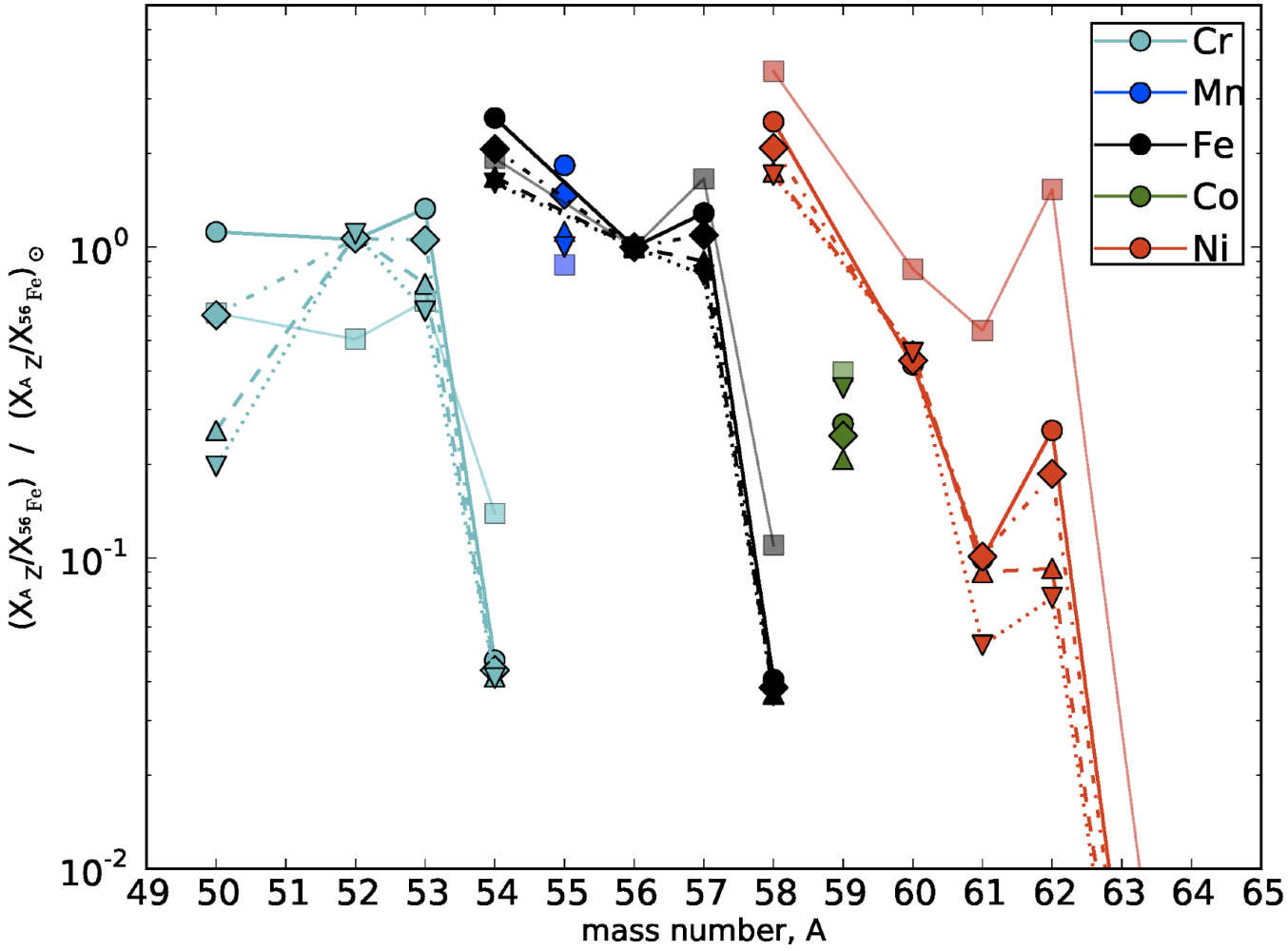

(Seitenzahl, Ciaraldi-Schoolmann, Röpke et al. 2013, MNRAS 429, 1156)

P-process isotope yields for solar metallicity s-process seeds for 2D DDT model

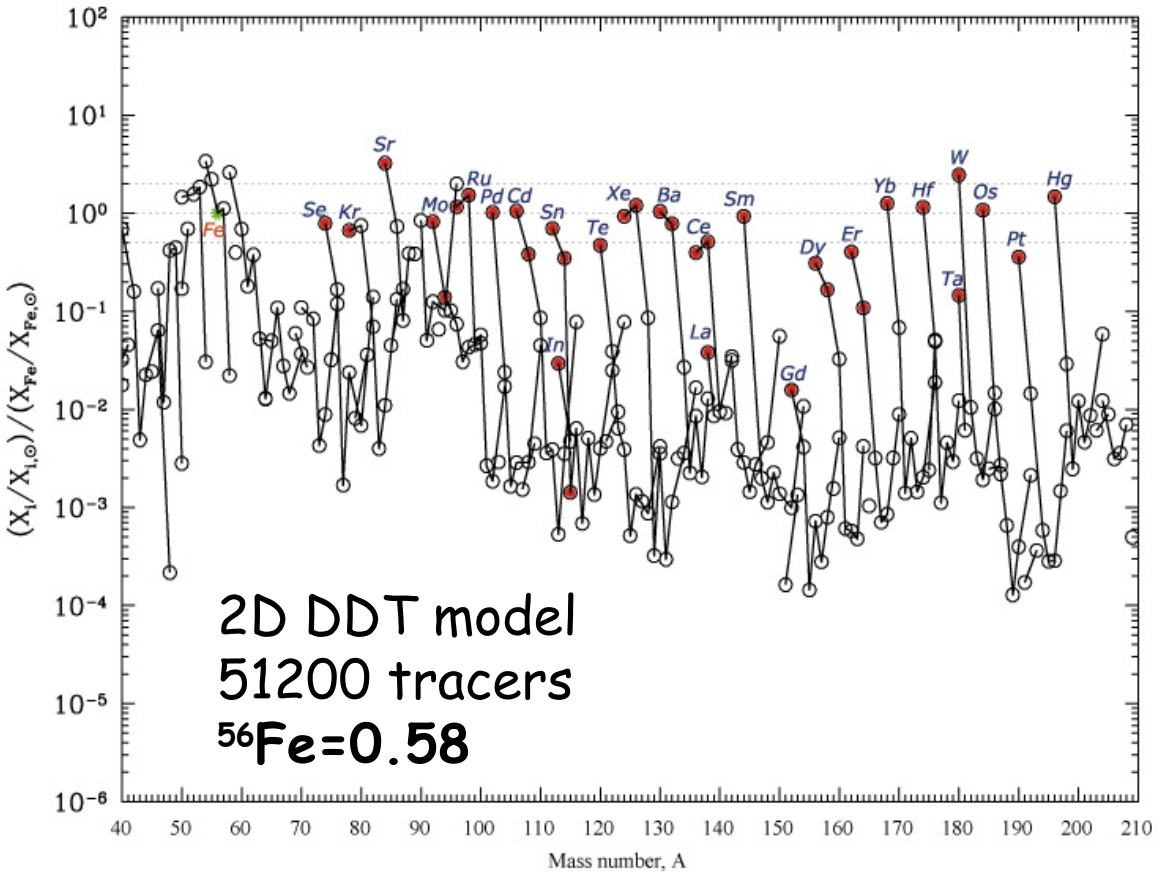

Nuclear reaction channel	Produced final isotope(%)
^{99}Ru(γ,n)^{98}Ru	69
^{99}Rh(γ,p)^{98}Ru	31
^{75}Se(γ,n)^{74}Se	100
^{97}Ru(γ,n)^{96}Ru	93
^{100}Pd(γ,α)^{96}Ru	7
^{95}Mo(γ,n)^{94}Mo	100
^{85}Sr(γ,n)^{84}Sr	100
^{79}Kr(γ,n)^{78}Kr	100
^{93}Mo(γ,n)^{92}Mo	76
^{96}Ru(γ,α)^{92}Mo	24
^{81}Kr(γ,n)^{80}Kr	75
^{87}Sr(γ,n)^{86}Sr	85
^{91}Zr(γ,n)^{90}Zr	66
^{96}Zr(n,γ)^{96}Zr	100
^{91}Nb(γ,p)^{90}Zr	33

Figure Courtesy of Claudia Travaglio

Primary nucleosynthesis yields due to fusion in low peak temperature trajectories

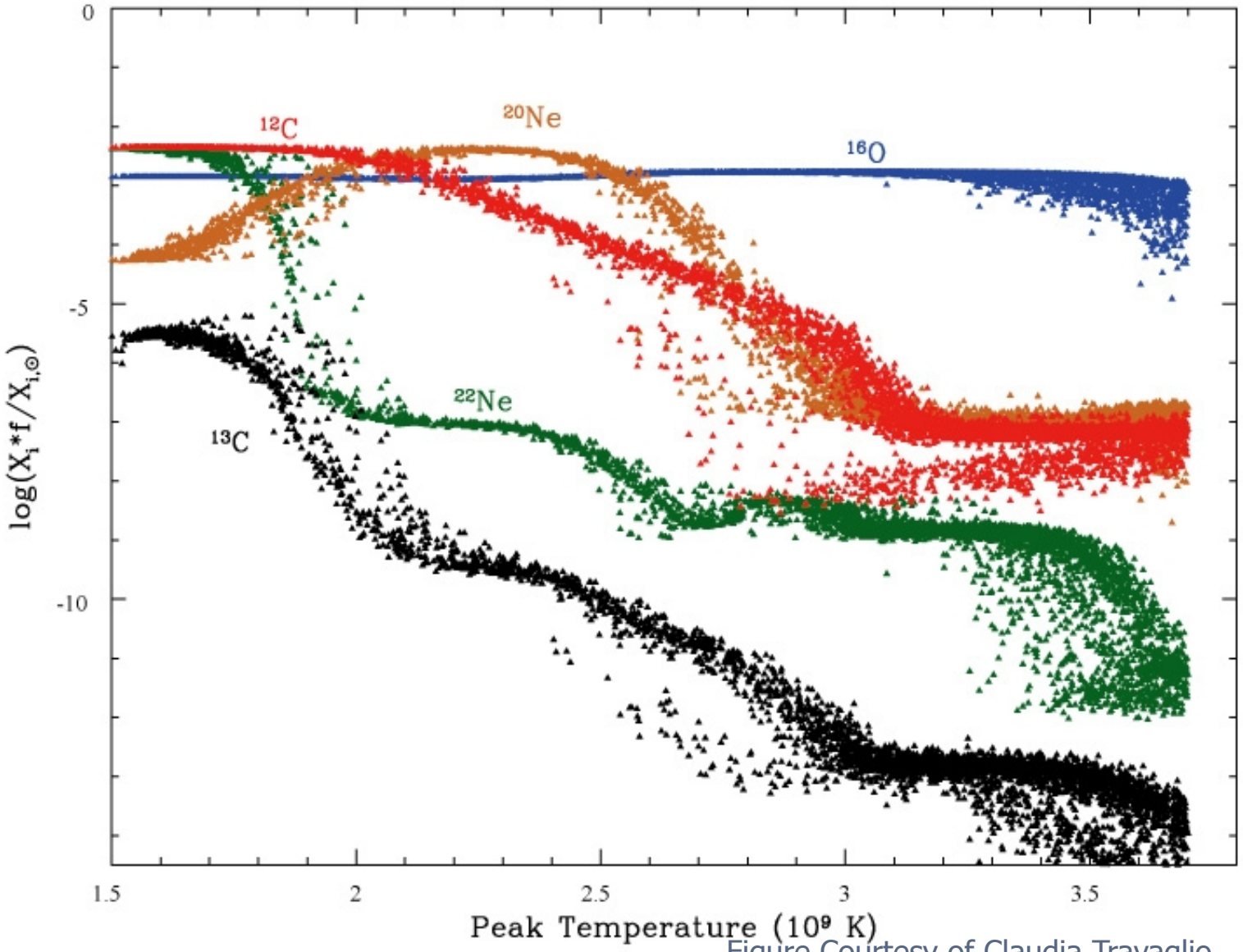

Figure Courtesy of Claudia Travaglio

Relative P-process abundances as a function of peak temperature DDT model

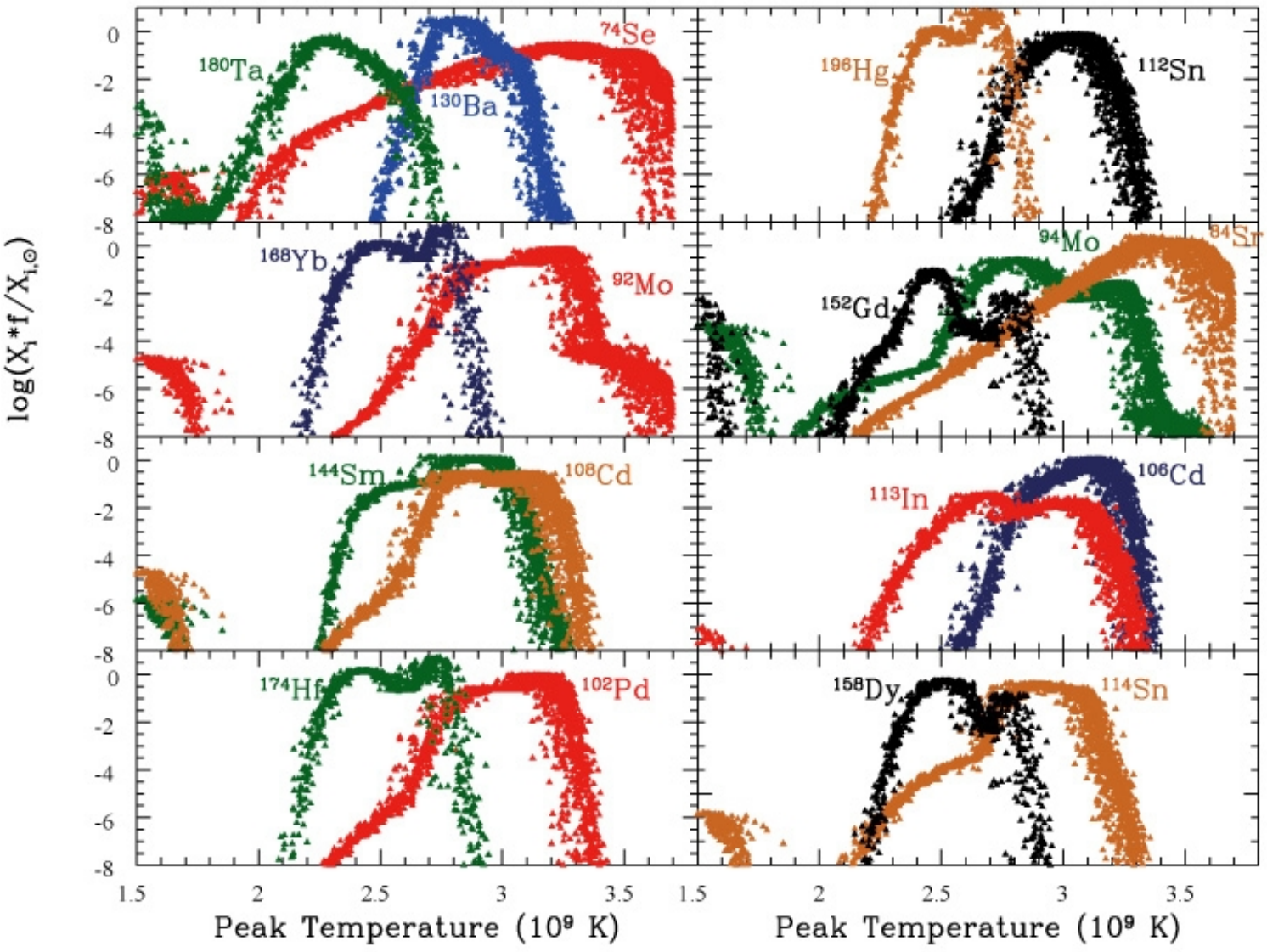

Figure Courtesy of Claudia Travaglio

M_{ch} delayed detonation vs. violent merger

	delayed detonation M_{Ch} WD	violent merger (1.1+0.9 $M_\odot$ WD)
^{56}Ni mass [$M_\odot$]	0.604	0.616
mass of ^{57}Ni and ^{57}Co [$M_\odot$]	1.88×10^{-2}	1.49×10^{-2}
mass of ^{55}Fe and ^{55}Co [$M_\odot$]	1.33×10^{-2}	3.73×10^{-3}

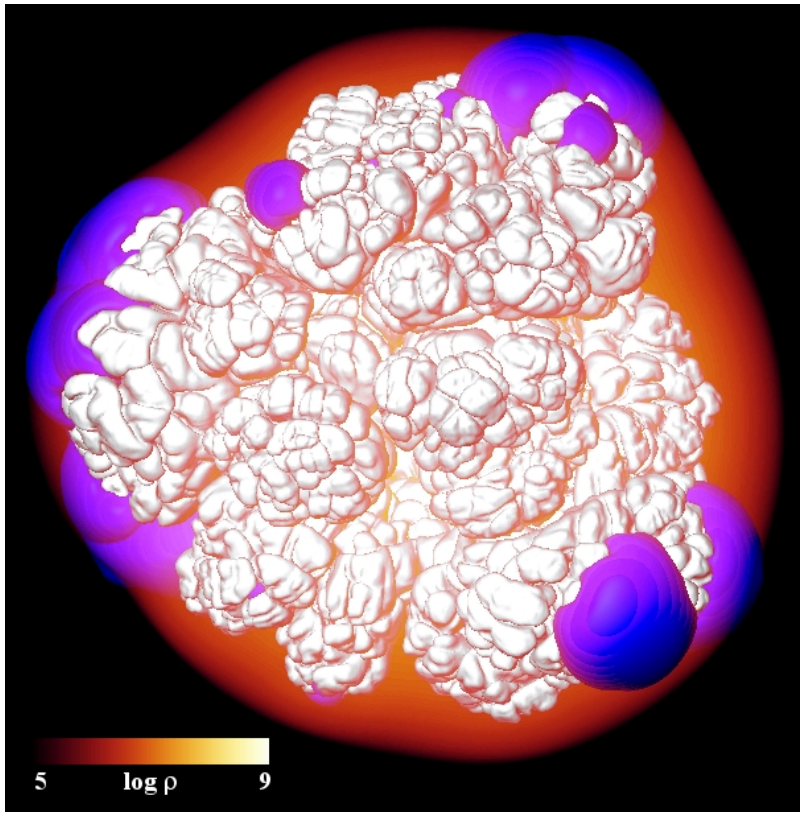

(Seitenzahl, Ciaraldi-Schoolmann, Röpke et al. 2013, MNRAS 429, 1156)

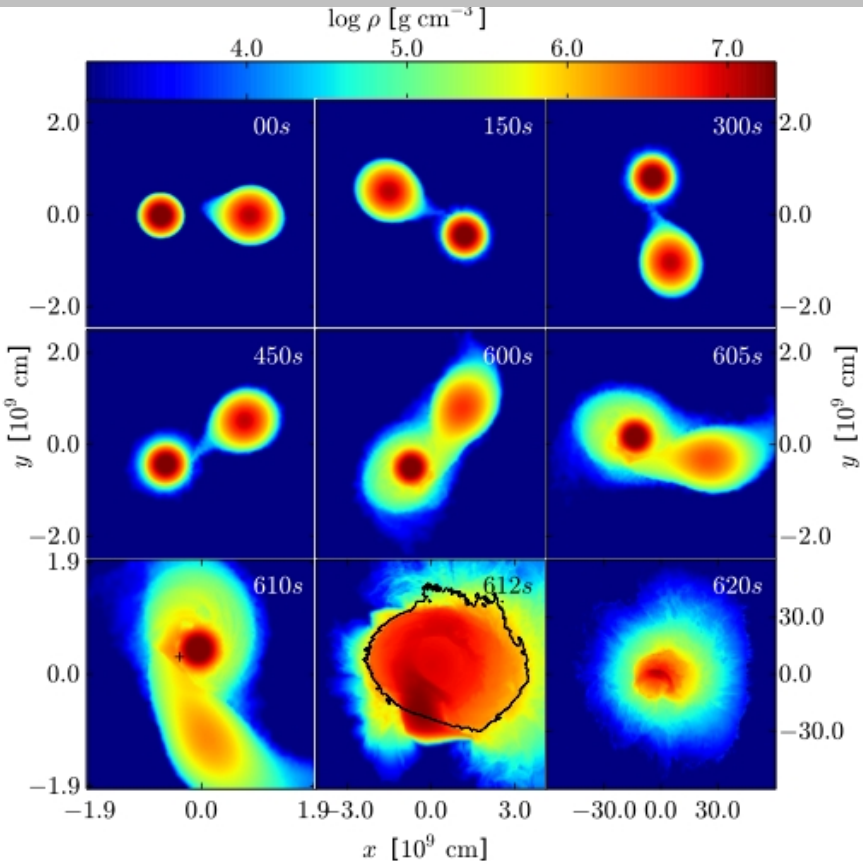

Pakmor et al. (2012) ApJ 747, 10

Spectrum of delayed-detonation and violent merger compared to SN 2011fe

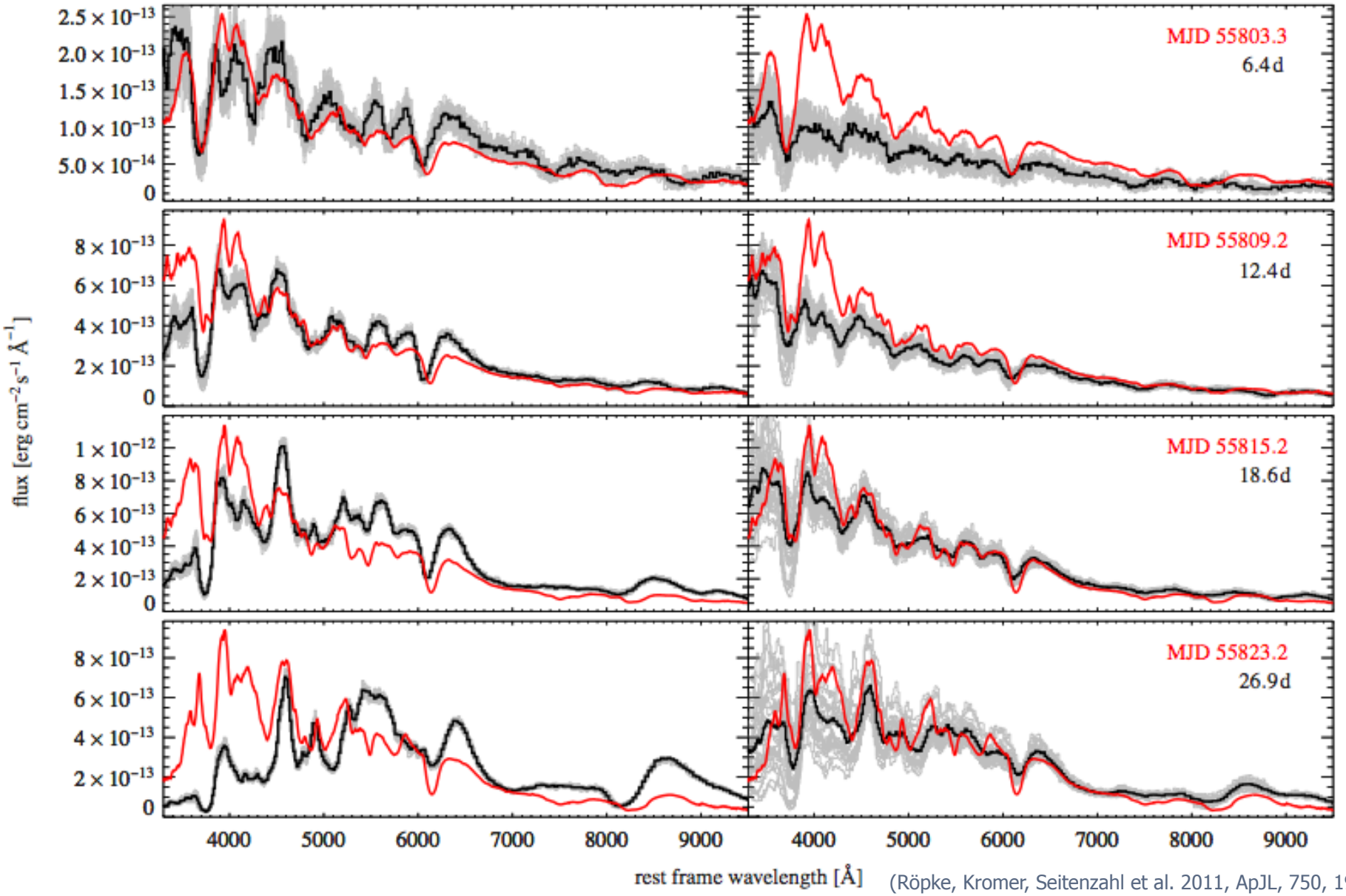

(Röpke, Kromer, Seitenzahl et al. 2011, ApJL, 750, 19)

Possible late light curves for SN 2011fe

- Merger and delayed-detonation models produce at equal ^{56}Ni yields somewhat different ^{57}Ni and very different amounts of ^{55}Co (due to different central densities). This provides an additional, independent way to distinguish the models.

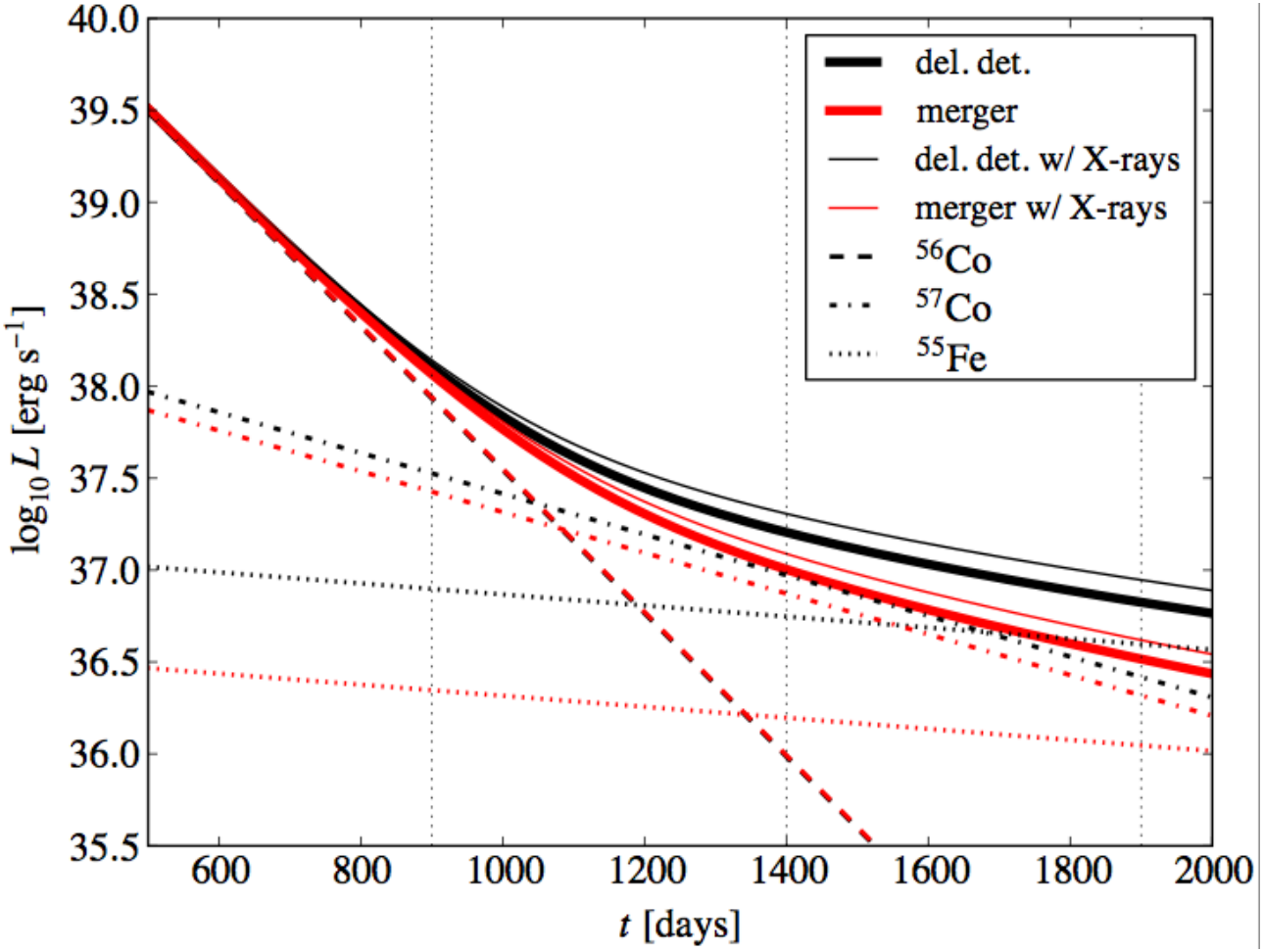

(Röpke, Kromer, Seitenzahl et al. 2011, ApJL, 750, 19)

Gamma ray light curves and spectra

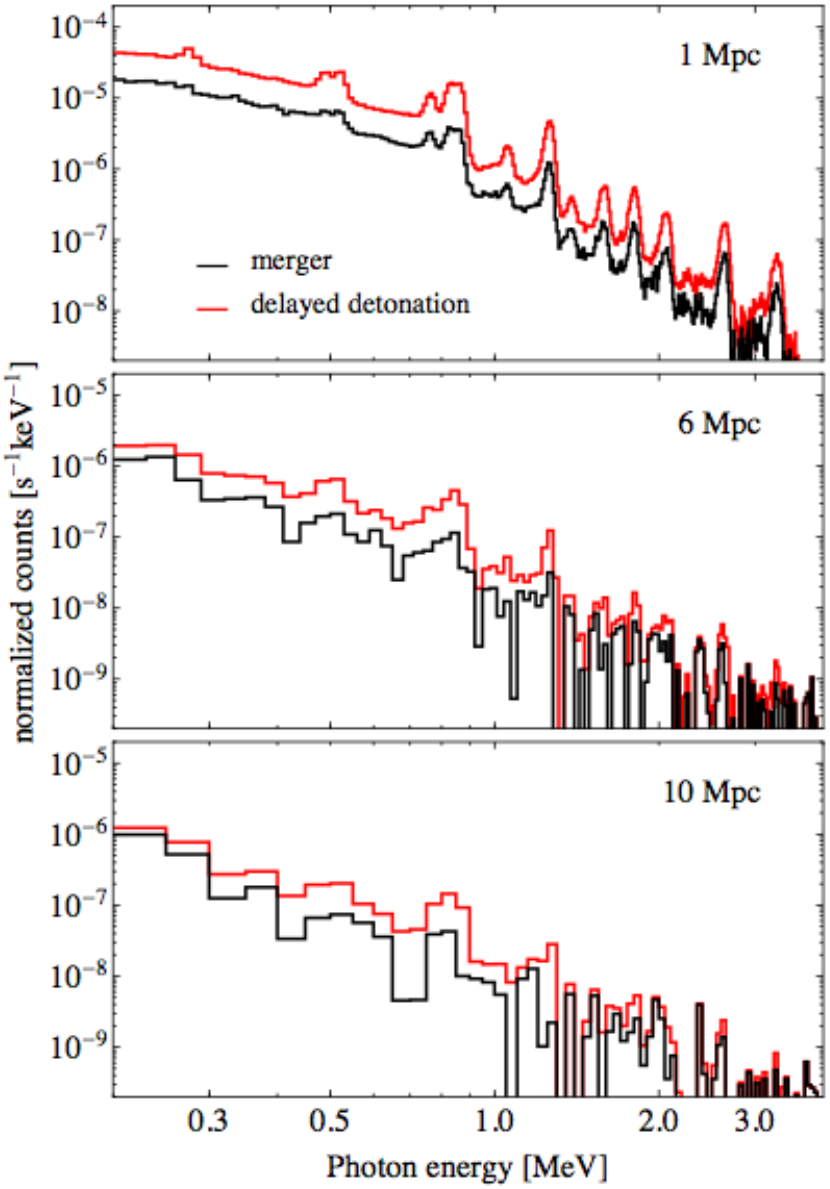

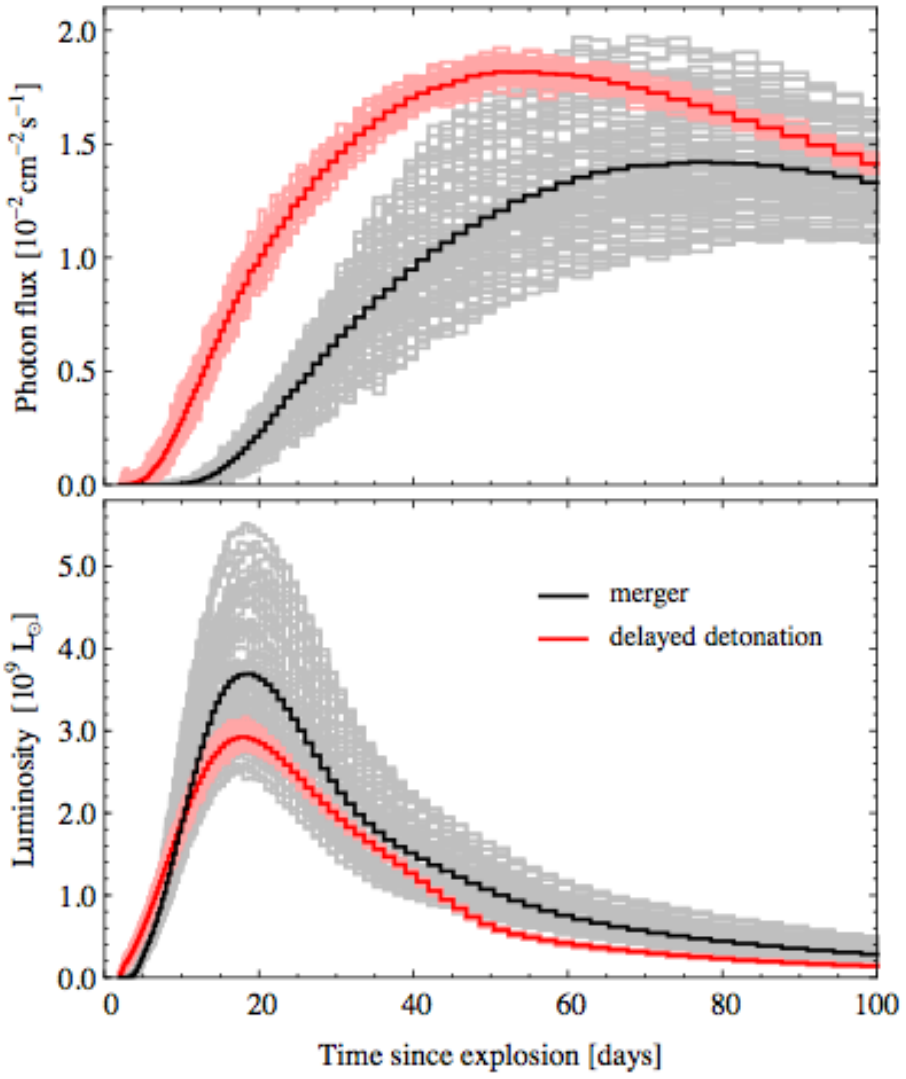

(Summa et al. 2013, submitted to A&A)

Predicted Mn Kα X-ray line for SNe Ia scenarios

Completely independent way of distinguishing competing explosion scenarios

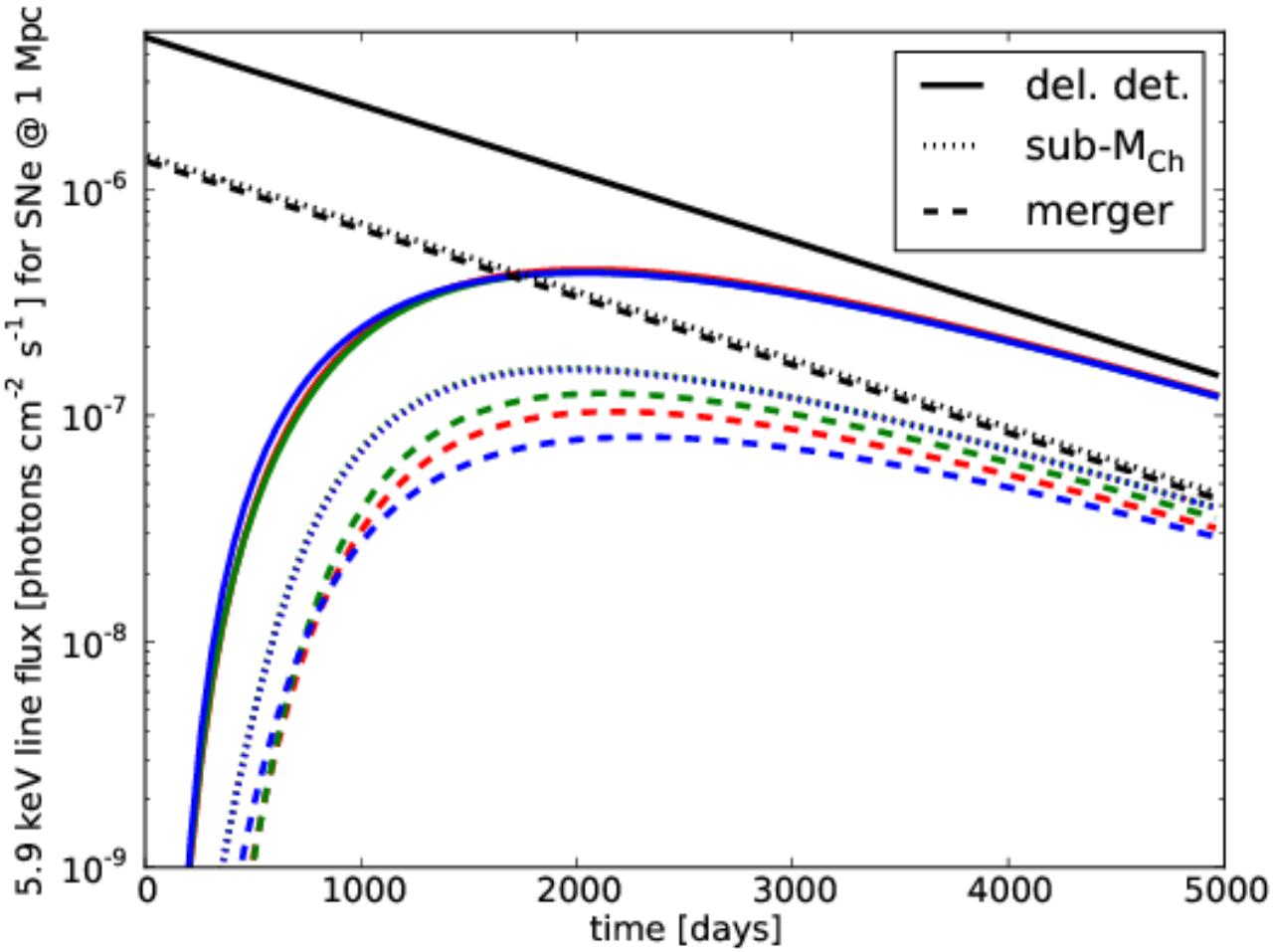

Seitenzahl et al. 2013, in preparation

RT calculation by S. Sim, Merger model by R. Pakmor, Sub-M_{Ch} model by M. Fink

Conclusions

- SNe Ia are important sources of Fe-group and p-nuclei.
- Detailed SN Ia nucleosynthesis essential for deriving synthetic observables, such as spectra and light curves.
- Sensitivity of nucleosynthesis to thermodynamic conditions can be used to distinguish explosion models.
- Community often still uses old W7 yields. Better to use updated W7 yields or, even better, our latest compilation of metallicity dependent 3D yields.